Global Ionospheric TEC Variations During January 10, 1997 Storm

C. M. Ho, A. J. Mannucci, U. J. Lindqwister, X. Pi, B.T. Tsurutani,
L. Sparks, B.A.Iijima, B. D. Wilson, M. J. Reyes, and I. Harris

Jet Propulsion Laboratory,
California Institute of Technology, Pasadena, California

To be submitted to Special Issue
in *Geophysical Research Letters*

Revised on October 30, 1997

Abstract: The ionospheric storm evolution process was monitored during the January 10, 1997 magnetic cloud event, through measurements of the ionospheric total electron content (TEC) from 150 GPS stations. The first significant response of the ionospheric TEC to the geomagnetic storm was at 0300 UT as an auroral/subauroral enhancement around the Alaskan evening sector. This enhancement then extended to both noon and midnight. Around 0900 UT, the enhancement at noon broke from the subauroral band and moved to lower latitudes. This dayside northern hemisphere enhancement also corresponded to a conjugate geomagnetic latitude enhancement in the southern hemisphere and lasted about 5 hours. At the same time, some large enhancements also appeared at around 40°S from afternoon to dusk, and then gradually shifted to nightside. At 1500 UT a large middle latitude enhancement appeared over Mexico and the southern US, and persisted until 2200 UT. These middle latitude enhancements were probably caused by the equatorward neutral wind which pushed the plasma up. On the basis of this assumption, the kinetic energy of the neutral wind which caused the middle latitude enhancement is estimated as ~4.1×10^9 Joules. This is about 0.03% of solar wind energy impinging on the magnetosphere and about 3% of the energy deposited on polar cap ionosphere. After 2000 UT, a negative phase gradually became stronger (especially in the southern hemisphere), although the northern subauroral enhancement persisted one more day. The entire ionosphere gradually recovered to normal on January 12. Thus, large middle latitude enhancements, equatorward motion of the dayside enhancement (probably related to a TID), the persistence of the subauroral enhancement, and the conjugate features at both hemispheres are the main characteristics of this storm.

Introduction

Using data from 12 SATLOC GPS stations which are nearly uniformly distributed over the US continent, we detected a significant ionospheric TEC disturbance in real time on January 10, 1997. The TEC data retrieved from these GPS receivers were transferred to our ionospheric storm monitoring facility with a latency of about 3 seconds. At around 1630 UT on that day, the TEC enhancement reached its maximum (~4.5m in L_1 band range delay) in the southern US area between Florida and Baja California as shown in Figure 1. This was an increase of more than 100% relative to the quiet time ionosphere. Within an hour, the data from 24 GPS stations distributed over the globe confirmed our finding of the enhancement. TEC data from more than 150 GPS stations arrived within 24 hours, generating more detailed global ionospheric TEC pictures.

During a geomagnetic storm, the solar wind energy deposited into the magnetospheric polar cap region will eventually be dissipated into the ionosphere and thermosphere. Meanwhile, various physical and energy transport processes within the ionosphere become extreme and more complicated [Mendillo, 1971; Essex et al., 1981; Fuller-Rowell et al., 1997; Buonsanto and Fuller-Rowell, 1997]. Data from a worldwide network of GPS sites make it possible to trace the energy flow dissipation and transportation processes in the ionosphere [Ho et al., 1996]. For the January 10 storm event, various measurements from distributed and clustered ground-based instruments and from space-borne experiments coordinated by the ISTP program have contributed to a comprehensive data set. As an important indicator of the ionospheric storm, TEC data measured from the GPS network also provide a valuable supplement to the solar wind-magnetosphere-ionosphere coupling study.

Measurements

The GPS network is a global monitoring system with the capabilities of near real-time data acquisition, uniform calibration and centralized processing/analysis. Global ionospheric maps (GIM) of TEC are derived from data from the GPS network which, as part of international GPS service (IGS), is a continuously operating network of GPS receivers distributed worldwide [Wilson et al., 1995; Mannucci et al., 1998]. The receivers collect data at 30 second intervals, making it possible to monitor high frequency variations of the ionosphere in near real-time. Dual-frequency signals broadcasting from GPS satellites are

received by more than 150 GPS receivers distributed around the world. On the basis of both time delay of the signals and carrier phases, the slant TEC along the line of sight between any pair of satellite and receiver are calculated. Under an assumption of a infinitesimal thin shell for the ionosphere with a fixed shell height, ionospheric TEC values are obtained through a vertical projection at the intersecting point of line of sight with the shell ionosphere. Assuming that there is a linear relation for TEC variations within each vertex, all instrumental biases are calculated at 642 vertices over the globe [Mannucci et al., 1998]. At any time and any location (latitude and longitude) the TEC values in the global maps may be obtained through direct measurements and linear interpolation. These assumptions will result in some errors. especially when teh ionosphere has large horizontal gradients. The typical error is within 5 TECU in most regions [Ho et al., 1997]. Differential ionospheric TEC maps are made by computing the percent change of storm-time TEC relative to TEC maps generated for quiet conditions, taking the quiet time variation (standard deviation) as a threshold. In this study, we have used 5 days (January 4 - 9, with low geomagnetic activity) of TEC averages as quiet time reference.

Results

On January 10, 1997, the spacecraft WIND, 85 R_e upstream of Earth, detected an interplanetary shock at 0055 UT. A magnetic cloud with strong southward B_z started at 0440 UT (see Lepping et al., Tsurutani et al., this issue). In response, a magnetic storm initial phase with a sudden commencement was seen after 01 UT. The storm main phase lasted from 06 to 10 UT and had a minimum Dst index of -81 nT. Then a slow recovery phase followed. However, this recovery process was interrupted by a large solar wind pressure pulse (> 40 nPa) at 01 UT of January 11. The Dst did not return to its normal recovery course until 07 UT on January 11.

The response of the ionospheric TEC signatures to the energy input in the magnetosphere, was first seen in the northern hemispheric high latitude at 03 UT. Two auroral/subauroral enhancements (> 100% increase relative to the quiet days) appeared respectively at Alaska (16 LT) and Greenland (midnight). Then the evening enhancement extended toward both noon and midnight.

At the same time, there was a deep depression area (< -60%) around the geomagnetic equator. This TEC depletion lasted about 4 hours. Slightly south of the equator, an enhancement appeared at the Atlantic anomaly region. In addition, around local noon (12 -

15 LT) an enhancement occurred at ~15°N. These features suggest that the magnetospheric convection electric field (or dawn-dusk electric field) probably played a role during this period. When the IMF turned southward, the enhanced electric field may have penetrated to the ionosphere before the shielding [Buonsanto and Foster, 1993; Pi et al., 1993]. In general, the dayside electric field will lift the equatorial ionospheric plasma, while on the nightside it will push the plasma down by E×B drift.

At about 0900 UT, in the northern hemisphere, the high latitude enhancement near the noon broke from the subauroral band and expanded from 60° to 40°N (in geomagnetic latitude: gm) around noon. While lower latitude part of the enhancements moved equatorward by about 20° in latitude, suggesting a traveling ionospheric disturbance (TID) signature, its higher latitude part corresponded to a conjugate enhancement in the southern hemisphere at the same geomagnetic latitude range (50°- 60° gm). This pair of enhancements lasted until 14 UT. However, the nightside enhancement appearing at northern subauroral latitudes corresponded to a conjugate depression in the southern hemisphere during the same period. During this period, some latitudinal structures (enhancements then depressions) were also seen.

In the southern hemisphere, after the conjugate enhancement appeared at subauroral latitudes, some large enhancements also occurred at around 40°S gm in the evening sector and then gradually shifted to the nightside. All enhancements in both hemispheres reached their maximum at about 12 UT as shown in Figure 2, then the southern hemisphere depressions gradually began. These depressions were mainly seen in the sector from post-midnight to morning; significant depressions were seen at 18 UT at 50°-70°S gm.

A noticeable feature occurred at northern middle latitudes at ~1400 UT. This was the large enhancement around Mexico and the southern US (20°-40° N gm, peaking at 19 UT) we mentioned earlier. This enhancement then shifted from morning to afternoon and persisted until 2200 UT. It neither exactly corotated with earth at the same geographic longitude, nor did it remain fixed at the same local time. The angular momentum of the neutral wind or TAD probably controlled this character. We have found that the Coriolis force often plays a dominant role when a neutral wind propagate from high latitude to low latitude [Ho et al., 1998].

On basis of the TEC variations, we can roughly estimate the energy which is transported from high latitude to low latitude within the ionosphere via the neutral wind, under certain

assumptions. We can assume that this regional TEC enhancement is solely caused by an average height change Δh (typically, ~30 km [Prolss et al., 1991]), even though it is possible that the entire winter hemispheric enhancements are caused by the composition changes due to global circulation changes as suggested by Field and Rishbeth [1997]. When the equatorward neutral wind pushes plasma up, at higher altitudes there are lower ion recombination rates and higher production rates. Thus this process only involves a conversion between kinetic energy and gravitational potential energy. From measured TEC changes we can deduce the energy in the ionosphere during the storm. The relation between the TEC changes (ΔTEC) and potential energy per unit area (ε_p) is

$$\varepsilon_p = m_i g \Delta TEC \Delta h = \gamma m_i g TEC_q \Delta h \qquad (1)$$

where γ is the change ratio, m_i is the ion mass, g is the acceleration due to gravity and TEC_q is the quiet time TEC value. By integrating over the entire enhancement area we can obtain the total potential energy (E_p) due to the upward motion of all plasma mass. Furthermore, we have the relation between plasma vertical speed V_d, and neutral wind speed u, at a middle latitude where its magnetic field inclination angle is I.

$$V_d = u \sin I \cos I \qquad (2)$$

Thus total kinetic energy (E_k) of the neutral winds which caused the middle latitude enhancement is

$$E_k = \frac{1}{2} M_n u^2 = E_p / \sin^2 I \cdot \cos^2 I \qquad (3)$$

where M_n is all neutral mass. Using the measured TEC enhancement rate and area from the TEC maps, we have estimated that the kinetic energy of the neutral wind was roughly 4.0×10^9 Joules.

This enegry can be compared with the solar wind energy deposited into the magnetosphere of the earth. For the solar wind with an average density of 6 cm^{-3} and velocity of 440 km/s during this interval, we obtain a solar wind energy of ~ 1.2×10^{13} Joules per second. Thus, the neutral wind kinetic energy in the ionosphere which causes the middle latitude TEC enhancement during the storm is only about 0.03% of the solar wind energy.

Figure 3 shows this middle latitude TEC enhancement. This figure also illustrates a standard TEC global pattern for a northern hemisphere winter ionospheric storm. In this global map there are two distinct features: a middle latitude enhancement around noon and an auroral/subauroral enhancement in the nightside. Although every ionospheric storm has a different character because of various competing factors, two types of structure are often seen. On the dayside, the equatorward neutral winds, driven by the high thermal pressure

of the polar atmosphere, propagate to lower latitudes, crossing the field lines. After a few hours, the winds arrive at middle latitudes where they have the maximum lifting effect on plasma. At low latitudes, because of the low dip angles of the field lines and rapid damping of the neutral winds against polarward heat diffusion, TEC effects caused by the neutral wind become less obvious. On the nightside, auroral/subauroral enhancements cover a latitude range of about 15°-20°. They are caused partially by an increase in the impacting ionization of energetic particle precipitation around the auroral oval, and partially by the equatorward displacement of the polarward wall of the middle latitude trough [Proless et al., 1991]. During this January 10 storm event, several substorms occurred which caused auroral surges. A correlation study between TEC enhancements and auroral illumination in the auroral latitude needs to be performed.

During the recovery phase, the northern hemispheric enhancements remained strong until the next day (January 11). We do not see any clear TEC effects due to the solar wind pressure pulse occurring between 01 - 04 UT. After 07 UT of Jan. 11, only the auroral/subauroral enhancement remained. The entire ionosphere gradually recovered to normal on January 12.

We show TEC variations at all latitude ranges during the three days of the storm in Figure 4. The percent changes relative to the quiet time profiles are calculated along the Greenwich meridian for both hemispheres. From the figure we can clearly see the ionospheric storm phases at different latitudes. Along this longitude the positive phase started three hours after the begining of the geomagnetic storm (in other sectors, such as Alaska, it may have started earlier). In the 60° - 80°N geomagnetic latitude band, the first peak is the dayside enhancement, while the second one shows the pre-midnight enhancement, whose rate exceeds 100%. At most latitudes, TEC enhancements reached their maximum between 12 - 16 UT. In the southern hemisphere high latitudes (60°-80°S) there is a clear negative phase, which started after 16 UT. At other latitudes, smaller negative phases started later. These TEC depressions may be attributed to the thermospheric circulation and composition changes after the storm driven phase [Fuller-Rowell et al., 1994].

Summary

Through GPS global measurements, we have seen the some significant morphological features for ionospheric TEC variations during the storm. The main characteristics are: first the appearance of an auroral/subauroral enhancement on the nightside, middle latitude

enhancements around noon appearing a few hours later, conjugate latitude enhancements in both hemispheres, and high latitude depletions during the recovery phase. Equatorward motion of the dayside enhancement from 60° to 40°N and between 09 and 13 UT is probably associated with a TID. The effect of the magnetospheric electric field on the equatorial ionosphere is seen after the IMF turns southward. The large middle latitude enhancements are caused by the equatorward neutral wind. The global ionospheric disturbances started and ended with auroral/subauroral enhancements in the northern hemisphere.

We have estimated the kinetic energy for the neutral wind as 4.0×10^9 Joules, based on the middle latitude TEC enhancements. It is about 0.03% of the solar wind energy flux impinging on the magnetosphere. However, compared with the electromagnetic and particle energies deposited in the polar cap ionosphere (assumed to be 1% of the solar wind energy), about 3% of them was converted to neutral wind kinetic energy in the middle latitude ionosphere.

These preliminary results need to be compared further with other measurements from ionosonde and satellites. Also a comparison with computer simulation will help us to understand the storm evolution process and the physics mechanism in detail.

Acknowledgments: We would like to thank Ron Lepping from Goddard Space Flight Center and Alan Lazarus from MIT for providing upstream IMF and solar wind data. The research conducted at the Jet Propulsion Laboratory, California Institute of Technology was performed under contract to the National Aeronautics and Space Administration.

References

Buonsanto, M.J., and T.J. Fuller-Rowell, Strides made in understanding space weather at Earth, *EOS Trans. AGU, 78,* 1, 1997.

Buonsanto, M.J., and J.C.Foster, Effects of magnetospheric electric fields and neutral winds on the low-middle latitude ionosphere during the March 20-21, 1990, storm, *J. Geophys. Res., 98,* 19133, 1993.

Essex, E.A., et al., A global response of the total electron content of the ionosphere to the magnetic storm of 17 and 18 June 1972, *J. Atmos. Terr. Phys., 43,* 293, 1981.

Field, P. R. and H. Rishbeth, The response of the ionospheric F2-layer to geomagnetic activity: an analysis of worldwide data, *J. Atmos. Solar Terr. Phys, 59, 163-180, 1997.*

Fuller-Rowell, T.J., et al., Response of the thermosphere and ionosphere to geomagnetic storms, *J. Geophys. Res., 99,* 3893, 1994.

Fuller-Rowell, T.J., et al., How does the thermosphere and ionosphere react to geomagnetic storms? *Magnetic Storms,* AGU Monograph, Edt by B.T.Tsurutani et al., 203, 1997.

Ho, C.M. et al., Global ionosphere perturbations monitored by the worldwide GPS network, *Geophys. Res. Letts., 23,* 3219, 1996.

Ho, C.M., et al., A comparative study of the ionospheric TEC measurements by GIM with Topex and Bent model, *Radio Science, 32,* 1499, 1997.

Ho, C. M., et al., Global Ionospheric TEC Perturbations Monitored by the GPS Global Network during Two Northern Hemisphere Winter Storms, *J. Geophys. Res., in press,* 1998.

Mannucci, A.J., B.D.Wilson, D.N.Yuan, C.M.Ho, U.J.Lindqwister and T.F.Runge, A global mapping technique for GPS-derived ionospheric TEC measurements, *Radio Sci.*, 1998, in press.

Mendillo, M., Ionospheric total electron content behavior during geomagnetic storms, *Nature, 234,* 23, 1971.

Pi, X., M. Mendillo, M.W.Fox, and D.N.Anderson, Diurnal double maxima patterns in the F region ionosphere: Substorm-related aspects, *J. Geophys. Res., 98,* 13677, 1993.

Prölss, G.W., et al., Ionospheric storm effects at subauroral latitudes: A case study, *J. Geophys. Res., 96,* 1275, 1991.

Wilson, B.D., A.J.Mannucci, and C.D.Edwards, Sub-daily northern hemisphere maps using the IGS GPS network, *Radio Sci., 30,* 639, 1995.

Figure Captions

Figure 1. A map showing the ionospheric TEC over the US continent on a scale of L_1 band (1.57542 GHz) range delay (1 TECU = 16.2 cm). The map was made from 12 SATLOC GPS stations (black dots) over the US continent. A strong TEC enhancement relative to the background occurred in the southern US during the storm.

Figure 2. A pair of polar view maps for both hemispheres. Absolute TEC values are shown for storm time 1200 - 1300 UT, January 10, 1997. At this time, all enhancements in both hemispheres have reached their maxima. The white circles represent expected storm-time auroral regions.

Figure 3. A differential ionospheric TEC map at 1800 - 1900 UT of storm time relative to the quiet time. The map is shown in a geomagnetic coordinates (geomagnetic latitude vs magnetic local time). Two distinct structures are auroral/subauroral enhancements at nightside and the middle latitude enhancement at dayside. This is a typical global pattern for ionospheric TEC variations a few hours after storm onset.

Figure 4. Percent changes of storm ionospheric TEC relative to quiet time at different latitude bands. The vertical solid line marks the start time of the storm main phase (0600 UT, Jan 10), while the dashed lines gives the local noon. The ionospheric storm positive and negative phases appear clearly at higher latitudes. At lower latitudes (<20°), the storm effect is less obvious.

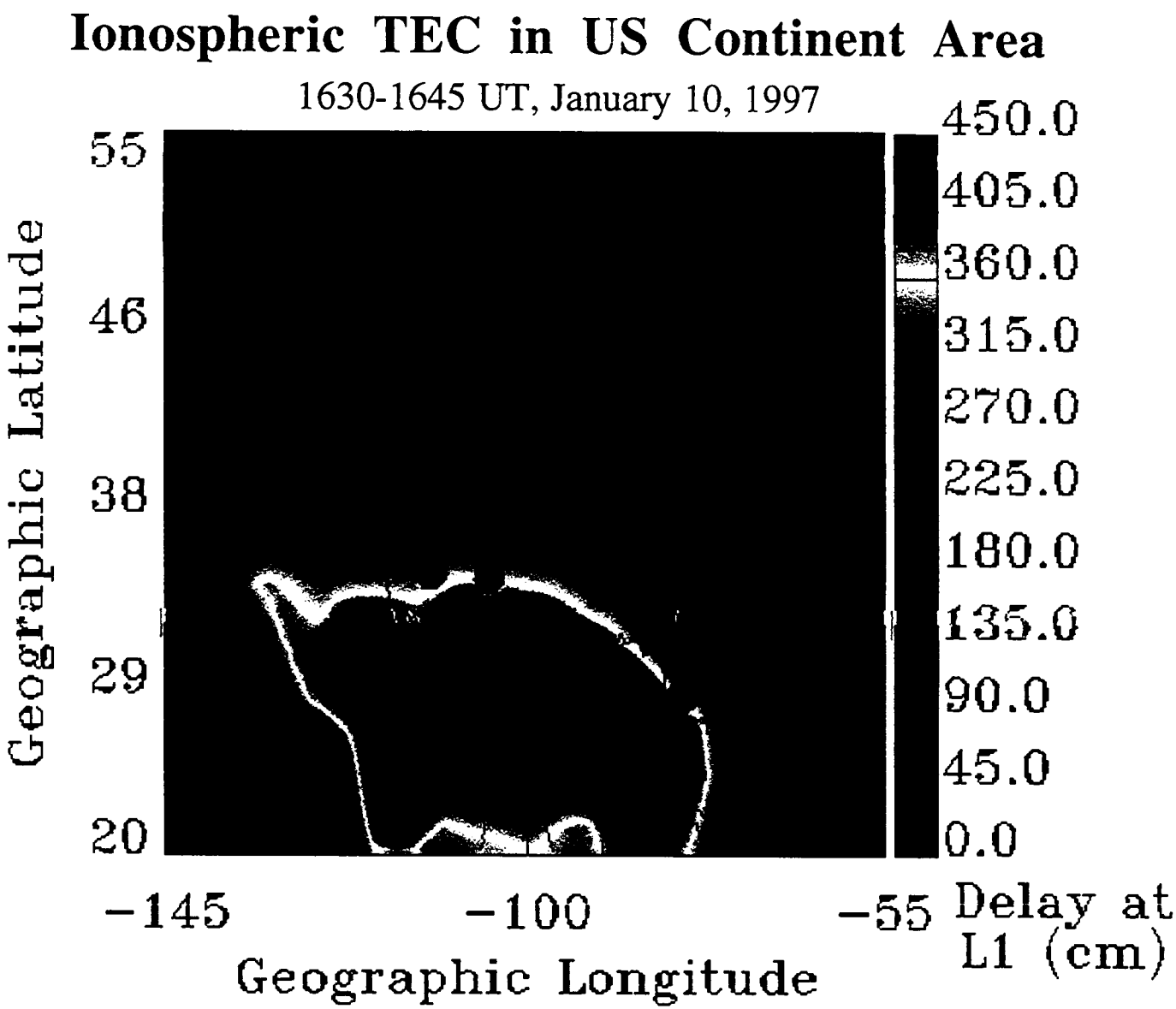
Ionospheric TEC in US Continent Area
1630-1645 UT, January 10, 1997
Geographic Latitude
55
46
38
29
20
−145
−100
−55
Geographic Longitude
450.0
405.0
360.0
315.0
270.0
225.0
180.0
135.0
90.0
45.0
0.0
Delay at L1 (cm)

Figure 1

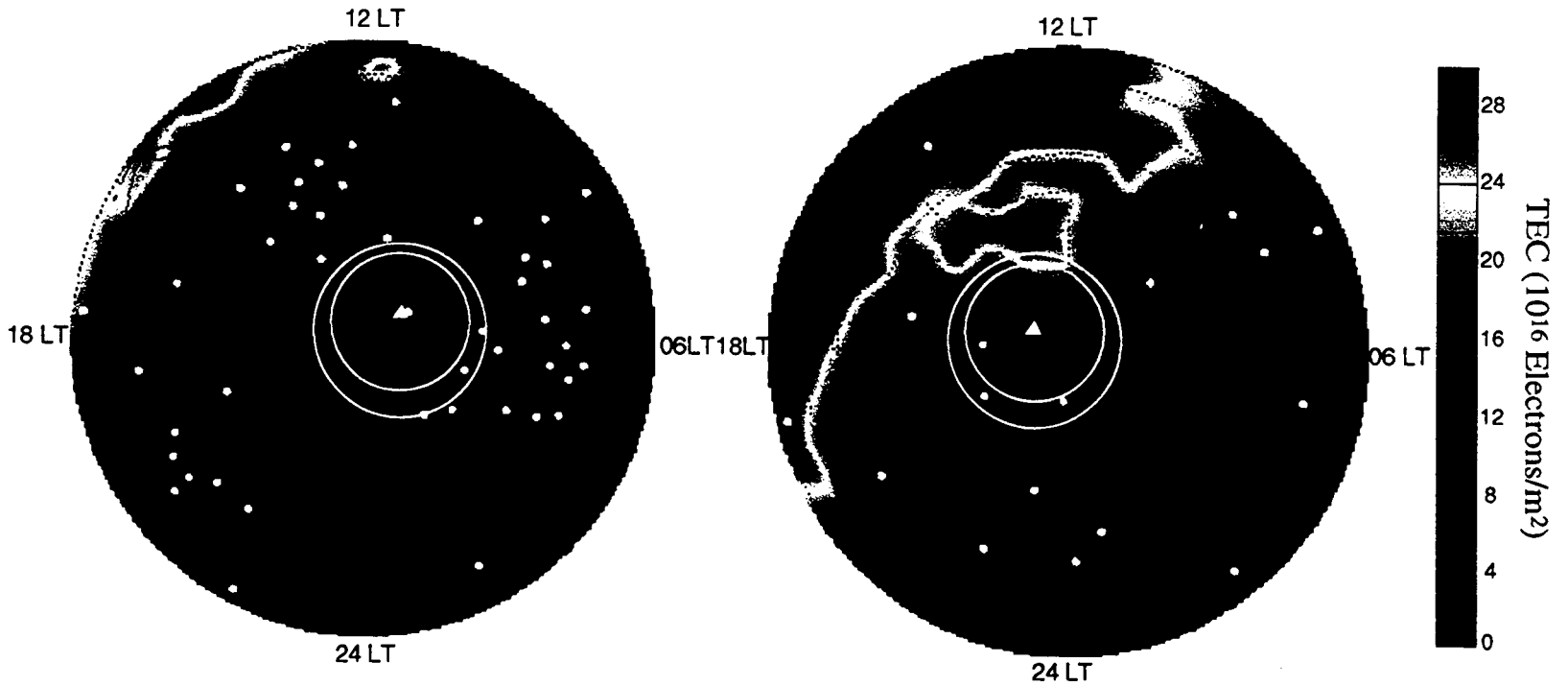
Absolute TEC Maps During Storm Time
12:00 - 13:00 UT, 01/10/1997
12 LT
18 LT
06LT
24 LT
Northern Hemisphere
12 LT
18LT
06 LT
24 LT
Southern Hemisphere
28
24
20
16
12
8
4
0
TEC (10¹⁶ Electrons/m²)

Figure 2

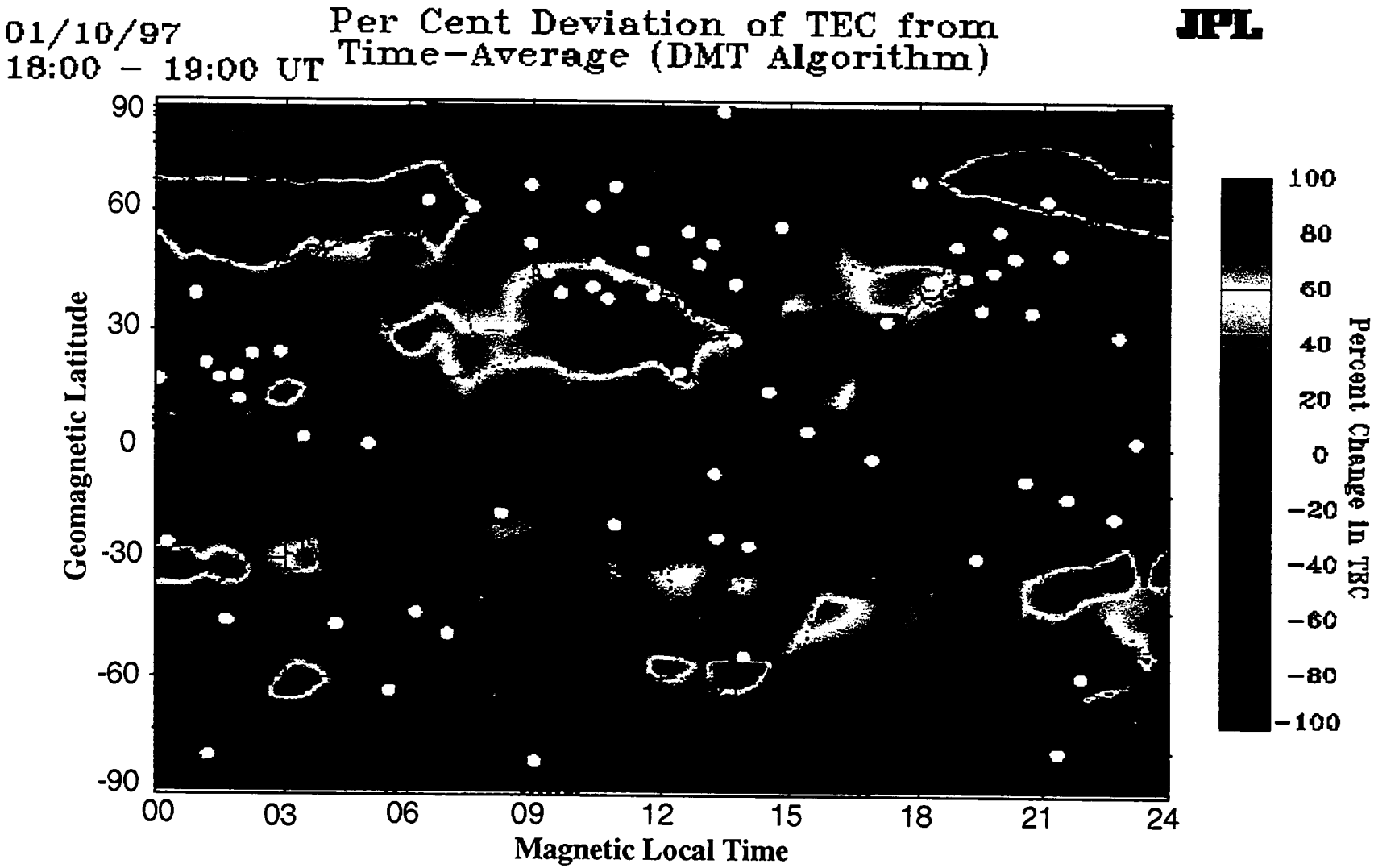
01/10/97
18:00 – 19:00 UT
Per Cent Deviation of TEC from Time-Average (DMT Algorithm)
JPL
90
60
30
0
-30
-60
-90
Geomagnetic Latitude
00
03
06
09
12
15
18
21
24
Magnetic Local Time
100
80
60
40
20
0
−20
−40
−60
−80
−100
Percent Change in TEC

Figure 3

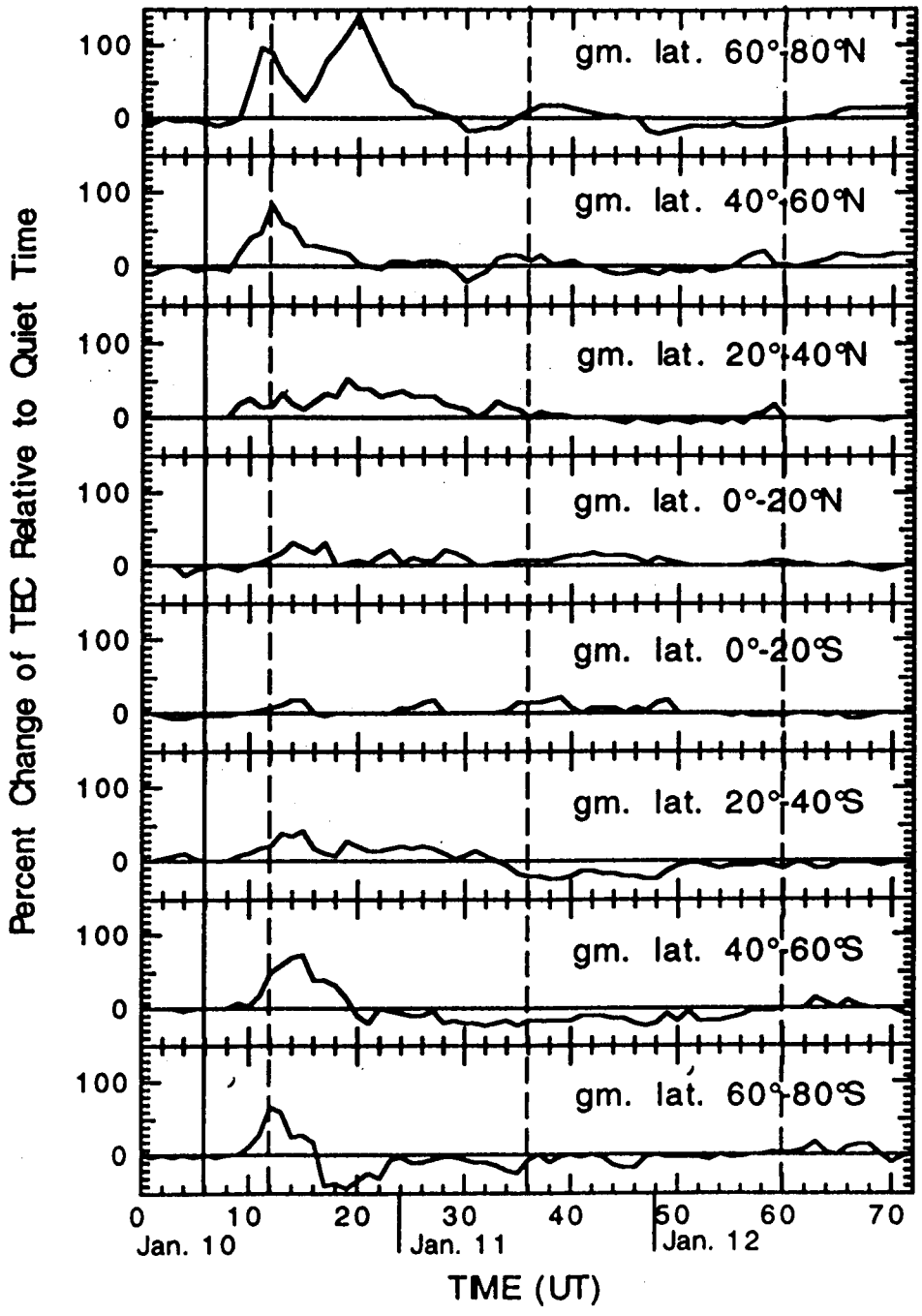
Percent Change of TEC Relative to Quiet Time
100
0
gm. lat. 60°-80°N
gm. lat. 40°-60°N
gm. lat. 20°-40°N
gm. lat. 0°-20°N
gm. lat. 0°-20°S
gm. lat. 20°-40°S
gm. lat. 40°-60°S
gm. lat. 60°-80°S
0
10
20
30
40
50
60
70
Jan. 10
Jan. 11
Jan. 12
TIME (UT)

Figure 4